Hindawi Publishing Corporation
International Journal of Photoenergy
Volume 2012, Article ID 405642, 7 pages
doi:10.1155/2012/405642

Research Article

Effects of Homogenization Scheme of TiO_2 Screen-Printing Paste for Dye-Sensitized Solar Cells

Seigo Ito,[1] Kaoru Takahashi,[1] Shin-ich Yusa,[2] Takahiro Imamura,[2] and Kenji Tanimoto[3]

[1] *Department of Electric Engineering and Computer Sciences, Graduate School of Engineering, University of Hyogo, 2167 Shosha, Himeji, Hyogo 671-2280, Japan*
[2] *Department of Materials Science and Chemistry, Graduate School of Engineering, University of Hyogo, 2167 Shosha, Himeji, Hyogo 671-2280, Japan*
[3] *Specialty Materials Research Laboratory, Nissan Chemical Industries, Ltd., 11-1 Kitasode, Sodegaurashi, Chiba 299-0266, Japan*

Correspondence should be addressed to Seigo Ito, itou@eng.u-hyogo.ac.jp

Received 15 October 2011; Revised 2 December 2011; Accepted 2 December 2011

Academic Editor: Jiaguo Yu

TiO_2 porous electrodes have been fabricated for photoelectrodes in dye-sensitized solar cells (DSCs) using TiO_2 screen-printing paste from nanocrystalline TiO_2 powder dried from the synthesized sol. We prepared the TiO_2 screen-printing paste by two different methods to disperse the nanocrystalline TiO_2 powder: a "ball-milling route" and a "mortal-grinding route." The TiO_2 ball-milling (TiO_2-BM) route gave monodisperse TiO_2 nanoparticles, resulting in high photocurrent density (14.2 mA cm^{-2}) and high photoconversion efficiency (8.27%). On the other hand, the TiO_2 mortal-grinding (TiO_2-MG) route gave large aggregate of TiO_2 nanoparticles, resulting in low photocurrent density (11.5 mA cm^{-2}) and low photoconversion efficiency (6.43%). To analyze the photovoltaic characteristics, we measured the incident photon-to-current efficiency, light absorption spectroscopy, and electrical impedance spectroscopy of DSCs.

1. Introduction

Dye-sensitized solar cells (DSCs) have been researched in the pursuit of a cost-effective solar generation system [1–3]. DSCs are composed of nanocrystalline-TiO_2 electrodes, sensitizing dyes, and electrolytes sandwiched between conducting substrates. The purpose of this work is to optimize the industrial fabrication methods of TiO_2-coating paste for nanocrystalline-TiO_2 electrodes. TiO_2 colloidal sol has produced DSCs with over 10% conversion efficiency [4]. DSCs fabricated using nanocrystalline-TiO_2 powders (P25, Degussa, by $TiCl_4$ fumed method) have over 9% conversion efficiency [5]. Thus, the TiO_2 sol methods have been investigated to produce DSCs with higher conversion efficiency [6, 7]. However, TiO_2 sol can aggregate and easily form precipitates, resulting in difficulties with long-term preservation. Alternatively, DSCs fabricated by using the TiO_2 powder method have lower conversion efficiency, but the powder without liquid improves long-term preservation and is suitable for transportation due to its light weight. Hence, it is important to find an industrial fabrication method to disperse nanocrystalline TiO_2 powder homogeneously. The purpose of this paper is to compare the characteristics and photovoltaic effects of DSCs using two TiO_2 homogenizing methods (ball milling and mortal grinding, named as TiO_2-BM and TiO_2-MG, resp.). The nanocrystalline TiO_2 powder was synthesized by sol gel method. As a result, an appropriate method for the industrial manufacture of nanocrystalline-TiO_2 electrodes has been identified.

2. Experimental

The methods used to fabricate TiO_2 paste from a TiO_2 particle source are shown in Figure 1. At first, TiO_2 nanoparticle was synthesized by peptization of titanium alkoxide, adjustment of pH, and hydrothermal reaction. The resulting TiO_2 nanoparticle was deionized, dried at 110°C, and heated at 380°C, resulting in anatase (d = 21 nm, by BET).

For the TiO_2 ball-milling paste (Figure 1, left side, named as "TiO_2-BM"), acetic acid and water were added to the

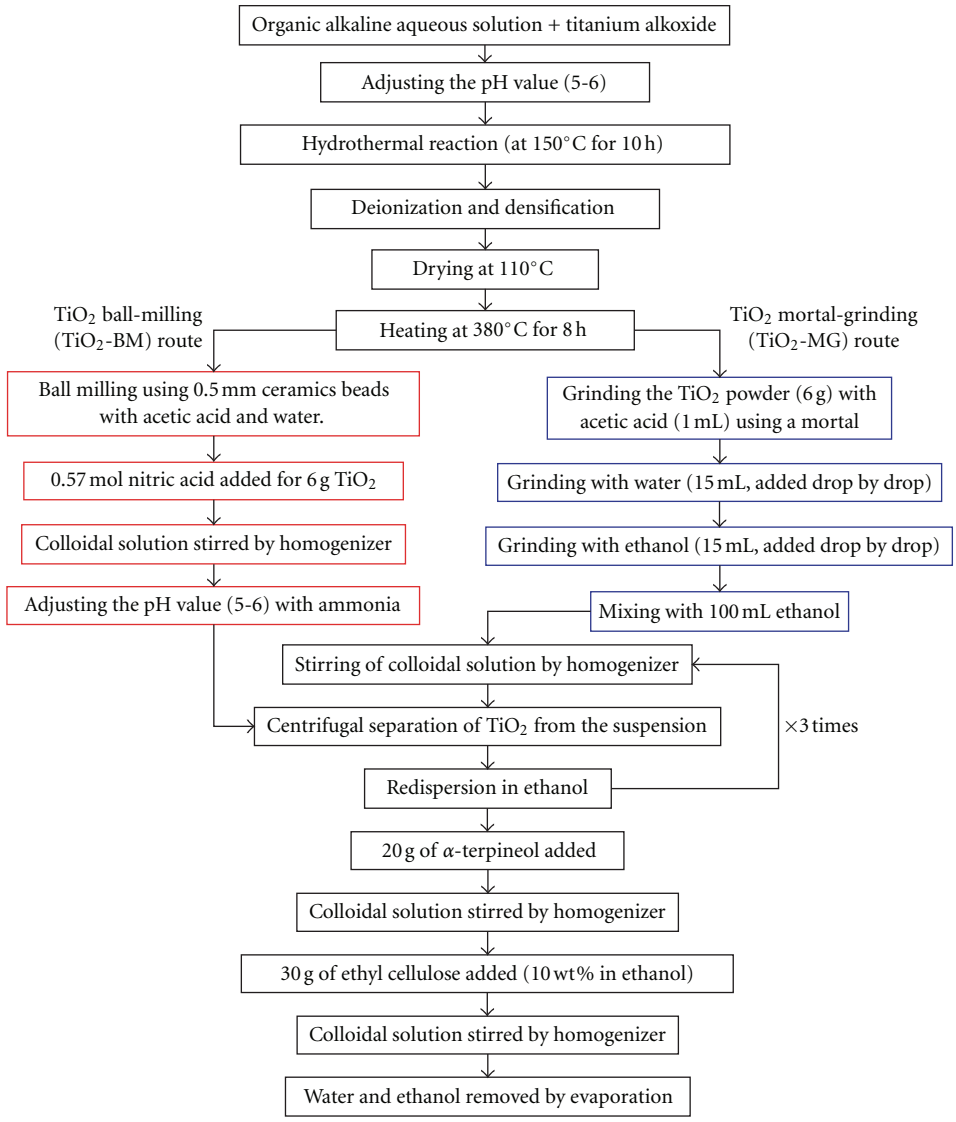

Figure 1: Fabrication methods of TiO_2 pastes.

nanocrystalline TiO_2 powder and mixed using ball milling with 0.5 mm ceramics balls. And then, nitric acid (0.57 mol for 6 g TiO_2) was added to the TiO_2 dispersion, and the pH value was adjusted to 5.7 using ammonium water. The resulting precipitation was centrifuged and washed with ethanol three times to remove nitric acid and water. After centrifugation, 20 g of α-terpineol (Tokyo Chemical Industries, Co. Ltd.) and 30 g of a mixture of two ethyl celluloses in ethanol (5 wt% of ethyl cellulose no. 46080 and 5 wt% of ethyl cellulose no. 86480, Tokyo Chemical Industries, Co. Ltd.) were added. The mixture was stirred by a magnet tip and sonicated using an ultrasonic horn (VC505, 500 W, Sonics & Materials Inc.). The contents in the dispersion were concentrated by using an evaporator at 35°C to remove ethanol and water.

For the TiO_2 mortal-grinding paste (Figure 1, right side, named as TiO_2-MG), the heated TiO_2 powder (6 g), acetic acid (1 mL), water (5 mL), and ethanol (15 mL) were mixed drop by drop in a mortar and grinded. The resulting mixture was transferred to a beaker and rinsed with 100 mL ethanol. The subsequent procedures were the same as those for TiO_2-BM paste.

To prepare the DSC working electrodes, F-doped tin oxide (FTO, Nippon Sheet Glass Co. Ltd., Japan) glass plates were first cleaned in a detergent solution using an ultrasonic bath for 15 min and then rinsed with tap water, pure water, and ethanol. After treatment in a UV-O_3 system for 18 min, the FTO glass plates were immersed into a 40 mM aqueous $TiCl_4$ *aq.* solution at 70°C for 30 min and washed with pure water and ethanol before drying. The plates were then repeatedly coated with the TiO_2 pastes (TiO_2-BM or TiO_2-MG) by screen printing and drying at 125°C, to a thickness of 17 μm. After drying at 125°C, a TiO_2 paste for a light-scattering TiO_2 film containing 400 nm anatase particles (PST-400C, CCIC-JGC, Japan) was deposited by screen printing to a thickness of 4-5 μm. The

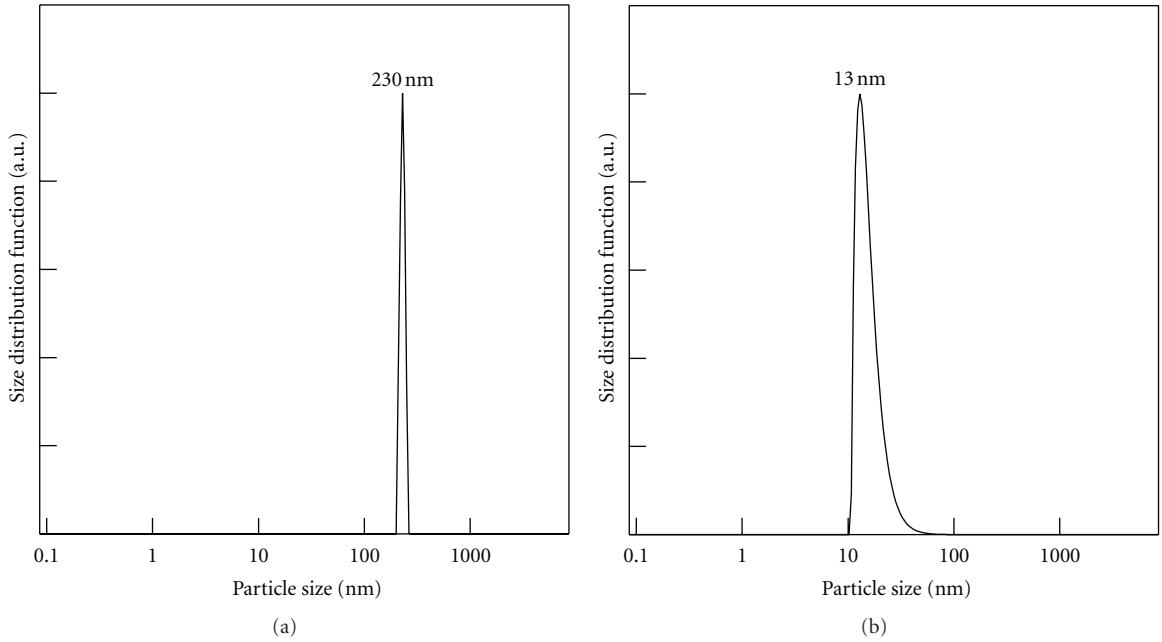

Figure 2: DLS measurements of TiO_2-MG (a) and TiO_2-BM (b) dispersions.

electrodes coated with the TiO_2 pastes were gradually heated under an air flow at 325°C for 5 min, 375°C for 5 min, 450°C for 15 min, and 500°C for 15 min. The sintered TiO_2 film was treated again with 40 mM $TiCl_4$ solution, as described above, rinsed with pure water and ethanol, and sintered again at 500°C for 30 min. After cooling to 80°C, the TiO_2 electrode was immersed into a 0.5 mM N-719 dye (Solaronix SA, Switzerland) solution in a mixture of acetonitrile and *tert*-butyl alcohol (volume ratio: 1 : 1) and kept at room temperature for 20–24 h to ensure complete sensitizer uptake.

To prepare the counter electrode, a hole was drilled in a FTO glass plate. The perforated sheet was washed with H_2O and a solution of 0.1 M HCl in ethanol and cleaned by ultrasound in an acetone bath for 10 min. After removing residual organic contaminants by heating in air for 15 min at 400°C, the Pt catalyst was deposited on the FTO glass by coating with a drop of H_2PtCl_6 solution (2 mg Pt in 1 mL ethanol), and heat treatment was carried out again at 400°C for 15 min. The additional Pt electrode content on FTO did not influence conversion efficiency. The Pt fabricated from H_2PtCl_4 was better than sputtered Pt films and metal Pt plates.

The dye-covered TiO_2 electrode and Pt-counter electrode were assembled into a sandwich-type cell and sealed with a hot-melt gasket of 25 μm thickness made of the ionomer Surlyn 1702 (DuPont) on a heating stage. The hole in the back of the counter electrode was covered with a hot-melt ionomer film (Bynel 4164, 35 μm thickness, DuPont) by using a hot soldering iron covered with fluorine-polymer film. A needle was used to make a hole in the hot-melt ionomer film. A drop of the electrolyte, a solution of 0.60 M 1-methyl-3-propylimidazolium iodide, 0.03 M I_2, 0.10 M guanidinium thiocyanate, and 0.50 M 4-*tert*-butylpyridine in a mixture of acetonitrile and valeronitrile (volume ratio: 85 : 15) was placed into the hole. The cell was put into a small vacuum chamber for a few seconds to remove internal air. Exposing the electrolyte to ambient pressure again caused the electrolyte to be driven into the cell, a method known as vacuum-back filling. Finally, the hole was covered with additional hot-melt ionomer film and a cover glass (0.1 mm thickness) and sealed using a hot soldering iron. The edge of the FTO plate outside of the cell was scraped slightly with sandpaper or a file for good electrical contact with the photovoltaic measurement setup. A solder (Cerasolza, Asahi Glass) was applied on each side of the FTO electrodes by an ultrasonic-soldering system.

Photovoltaic measurements were conducted with an AM 1.5 solar simulator (100 mW cm^{-2}, Yamashita Denso Co. Ltd., Japan). The power of the simulated light was calibrated by using a reference Si photodiode equipped with an IR-cutoff filter (BS520, Bunko Keiki Co. Ltd., Japan) in order to reduce the mismatch in the region of 350–750 nm between the simulated light and AM 1.5 to less than 2% [8, 9]. I-V curves were obtained by applying an external bias to the cell and measuring the generated photocurrent with a digital source meter. Reflecting absorbance, incident photon-to-current efficiency (IPCE), and electrical impedance were measured on Lamda 750 (Perkin Elmer), CEP-2000 (Bunkou Keiki Co. Ltd., Japan), and SP-150 (Bio-Logic) apparatuses, respectively.

3. Results and Discussion

Dynamic light scattering (DLS) measurements of each paste diluted in ethanol are shown in Figure 2. It was clear that the TiO_2-MG paste contained large TiO_2 aggregates, but the TiO_2-BM paste contained monodispersed TiO_2 particles.

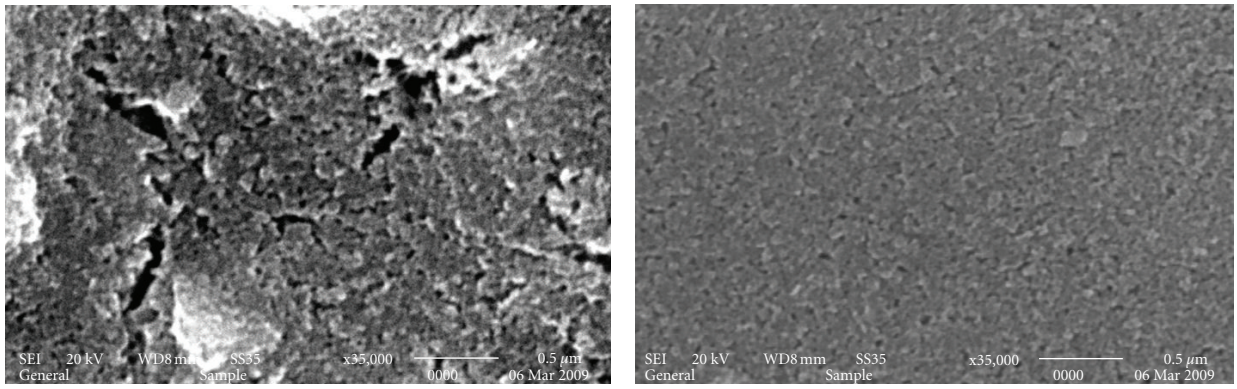

(a) (b)

Figure 3: Surface structures of nanocrystalline-TiO_2 layer made using the TiO_2-MG paste (a) and the TiO_2-BM paste (b). Magnification is ×35,000. Each scale bar is 500 nm.

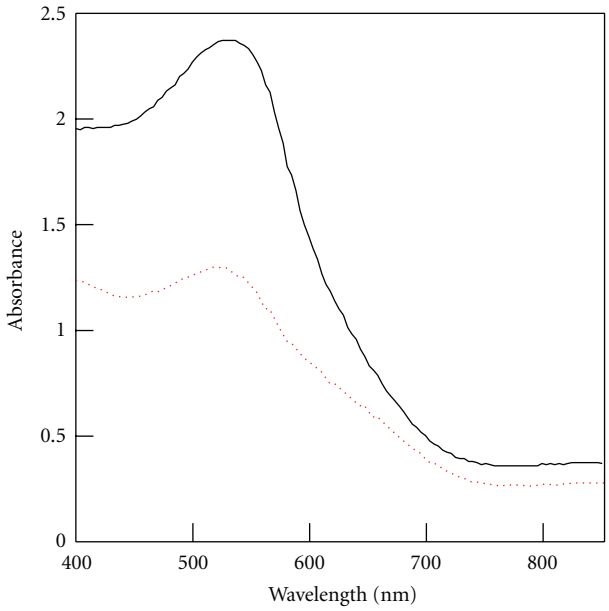

Figure 4: Absorbance spectra of nanocrystalline-TiO_2 electrodes with a sensitizing dye (N719): TiO_2-BM paste (solid line) and TiO_2-MG paste (dotted line).

Although the resulting size of a TiO_2 particle (Figure 2(b)) was smaller than that obtained by BET measurement (21 nm), the results were reliable enough to investigate the manner of dispersion.

The surface morphology of each screen-printed TiO_2 paste (Figure 3) showed that the TiO_2-MG paste contained large TiO_2 aggregates and cracks, but the TiO_2-BM paste gave a smooth surface. Hence, the morphology was projected the evaluation by using DLS measurements (Figure 2).

Figure 4 shows the reflectance-absorption spectra of dye-adsorbed nanocrystalline-TiO_2 electrodes from TiO_2-BM and TiO_2-MG pastes. The electrodes prepared from TiO_2-BM paste absorbed the incident light more effectively than those obtained from TiO_2-MG paste. Since the surface morphology was smooth and flat (Figure 3(b)), the electrodes from TiO_2-BM paste were transparent and the incident light was introduced deeply into the nanocrystalline-TiO_2 electrodes and largely absorbed. On the other hand, the large aggregates and cracks in nanocrystalline-TiO_2 electrodes from TiO_2-MG paste (Figure 3(a)) scattered the incident light and reflected it without absorption. Aggregates that formed during the drying process from the dispersion of TiO_2 could not be redispersed using the mortal grinding and ultrasonic homogenization.

The amount of adsorbed dye was confirmed by desorption from the nanocrystalline-TiO_2 electrodes using a 0.01 M NaOH *aq.* solution. The nanocrystalline-TiO_2 electrodes (17 μm thickness) from TiO_2-BM and TiO_2-MG pastes adsorbed 1.5×10^{-7} mol cm^{-2} and 6.5×10^{-8} mol cm^{-2}, respectively. Hence, it was confirmed that the nanocrystalline-TiO_2 electrodes from TiO_2-BM paste adsorbed double the amount of dye compared with those from TiO_2-MG paste, due to the high dispersion of TiO_2 nanoparticles in the TiO_2-BM paste.

In order to confirm the effect by human eyes, the photographs of DSCs were shown in Figure 5. It was very clear that TiO_2-BM was very dark purple color, on the other hand, TiO_2-MG was very light pink color, which means that DSC with TiO_2-BM absorbs light effectively, but TiO_2-MG cannot absorb light so much.

The IPCE spectra and photo I-V curves of DSCs using nanocrystalline-TiO_2 electrodes are shown in Figures 6 and 7, respectively. Projecting the results of Figures 4 and 5, the IPCE and photocurrent density of DSCs from TiO_2-BM paste were greater than those from TiO_2-MG paste. The photovoltaic results are summarized in Table 1. The photoconversion efficiency using the TiO_2-BM paste was higher by 29% compared with the TiO_2-MG paste. However, considering the large difference of light-absorbing effect (Figures 4 and 5), it was surprising that the difference of IPCE value and photocurrent was not so much. Hence, it was considered that the light diffusion and trapping effect in

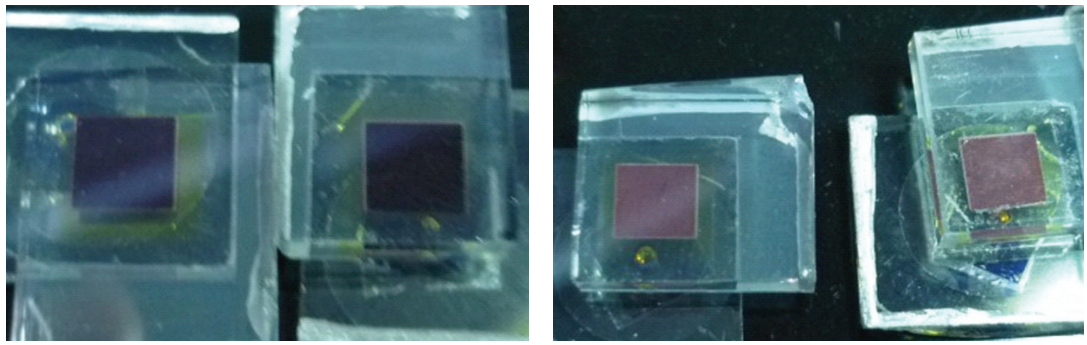

(a) (b)

Figure 5: Photographs of DSCs using TiO_2-BM (a) and TiO_2-MG (b).

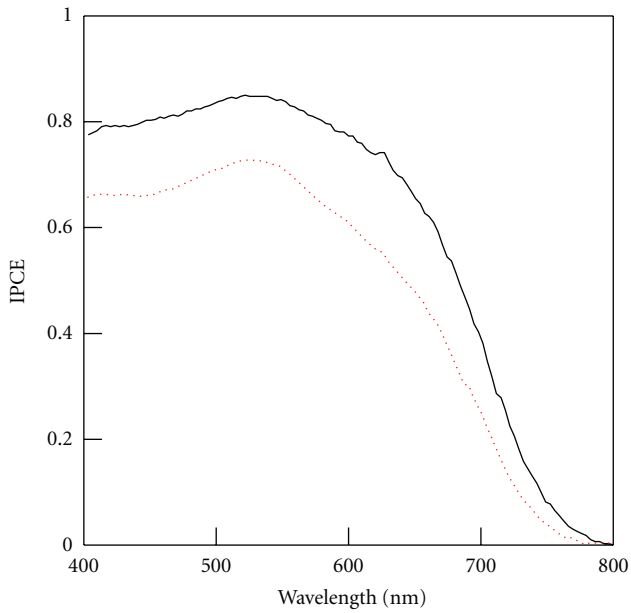

Figure 6: Incident photon-to-current conversion efficiency (IPCE) spectra of DSCs: TiO_2-BM paste (solid line), TiO_2-MG paste (dotted line).

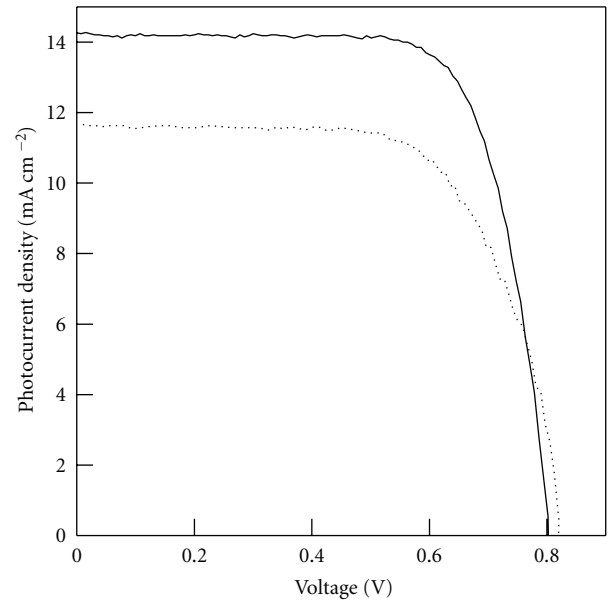

Figure 7: Photo I-V curve of DSCs under 100 mA cm^{-2} (AM 1.5): TiO_2-BM paste (solid line), TiO_2-MG paste (dotted line). The active areas of DSCs were 5×5 mm^2.

TiO_2-MG electrode would be significant to improve the photovoltaic effects. These phenomena might be projected the variation of mesoporous structures in the nanocrystalline-TiO_2 electrodes, which can be confirmed using the measurements results of the specific surface area and pore-size distributions [10, 11].

Figure 8 shows the electrical impedance spectra of DSCs. The center semicircles indicating the impedance of the interface between dyed TiO_2 and the electrolyte [12] were analyzed using an equivalent circuit (Figure 9) [3]. The results are summarized in Table 2. Although the series resistances (R_s) were the same, the constant phase element (CPE, showing the capacitance) of TiO_2-BM paste was greater by 20% than that of TiO_2-MG paste, and the parallel resistance (R_p) of TiO_2-MG paste was twice that of TiO_2-BM paste. The large CPE of the TiO_2 electrodes prepared from TiO_2-BM paste suggested a larger surface area than that obtained from TiO_2-MG paste, which resulted in greater dye adsorption and larger photocurrent density. Due to the large R_p of TiO_2-MG paste, the charge lifetime in DSCs ($\tau = R_p \times \text{CPE}$) from TiO_2-MG paste was greater than that from TiO_2-BM paste, thus suggesting a higher open-circuit photovoltage (20 mV).

Table 1: Photoelectric characteristics of DSCs fabricated using TiO_2-MG paste and TiO_2-BM paste. Each data was the average of three DSCs.

	TiO_2-MG	TiO_2-BM
J_{sc} [mA cm^{-2}]	11.5 ± 0.1	14.2 ± 0.01
V_{oc} [V]	0.821 ± 0.006	0.798 ± 0.001
FF	0.682 ± 0.03	0.731 ± 0.04
η [%]	6.43 ± 0.1	8.27 ± 0.08

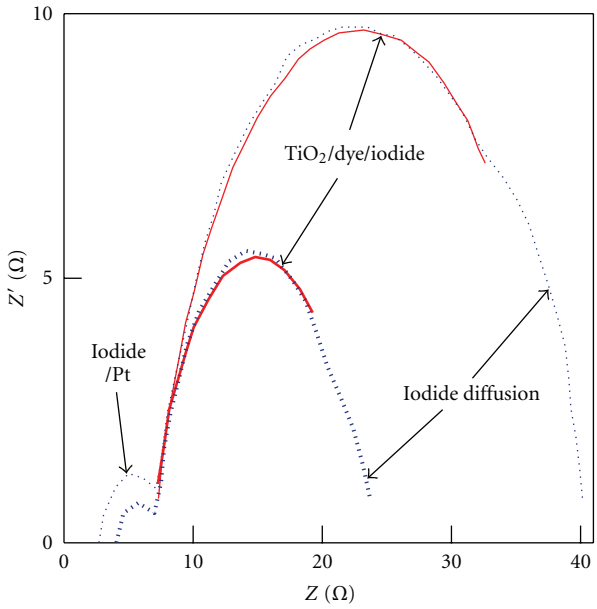

Figure 8: Electrical impedance spectra of DSCs under irradiation (100 mW cm^{-2}, AM 1.5): TiO_2-BM paste (thick-dotted line), TiO_2-MG paste (thin-dotted line). Each solid curve shows the fitting results.

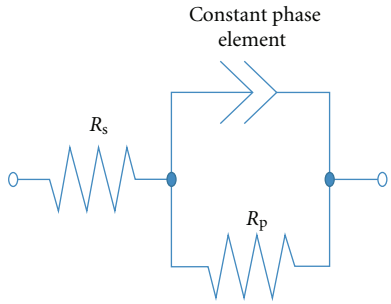

Figure 9: An equivalent circuit for analysis of TiO_2 electrodes in DSCs.

Table 2: Electrochemical impedance components from Figure 8.

	R_s [Ω]	CPE [F]	R_p [Ω]
TiO_2-MG paste	12.60	1.205×10^{-3}	26.12
TiO_2-BM paste	12.79	1.435×10^{-3}	12.77

4. Conclusion

This work demonstrated a comparison of different dispersion methods of fabricating coating paste for nanocrystalline-TiO_2 electrodes in DSCs. By using the same source of nanocrystalline TiO_2 powder, it was confirmed that the paste using mortal grinding (TiO_2-MG) produced a lower photocurrent and lower photoconversion efficiency compared using ball milling (TiO_2-BM). Large TiO_2 aggregates were produced during the drying process which caused a deterioration of dye adsorption and light penetration and resulted in a significant reduction in photocurrent density. Aggregates resulting from mortal grinding could not be redispersed by using an ultrasonic homogenizer with acid and polymer. Since powder materials can give the benefit for the manufacture of DSCs about transportation and preservation of nanocrystalline TiO_2, this ball milling method of dispersing TiO_2 nanoparticles from the dried powder is significant progress toward a cost-effective photovoltaic system. We hope that the results of this paper contribute to the industrial application of DSCs.

Conflict of Interest

The authors declare no conflict of interest.

Acknowledgments

The FTO glass plates and the glue films (Surlyn and Bynel) were provided by Nippon Sheet Glass Co. Ltd. and Tamapoly Co. Ltd., respectively. The IPCE spectra were measured on a system at Osaka University (Professor S. Yanagida and Dr. K. Manseki).

References

[1] B. O'Regan and M. Grätzel, "A low-cost, high-efficiency solar cell based on dye-sensitized colloidal TiO_2 films," *Nature*, vol. 353, no. 6346, pp. 737–740, 1991.

[2] M. Grätzel, "Photoelectrochemical cells," *Nature*, vol. 414, no. 6861, pp. 338–344, 2001.

[3] S. Ito, S. M. Zakeeruddin, P. Comte, P. Liska, D. Kuang, and M. Grätzel, "Bifacial dye-sensitized solar cells based on an ionic liquid electrolyte," *Nature Photonics*, vol. 2, no. 11, pp. 693–698, 2008.

[4] S. Ito, T. N. Murakami, P. Comte et al., "Fabrication of thin film dye sensitized solar cells with solar to electric power conversion efficiency over 10%," *Thin Solid Films*, vol. 516, no. 14, pp. 4613–4619, 2008.

[5] S. Ito, P. Chen, P. Comte et al., "Fabrication of screen-printing pastes from TiO_2 powders for dye-sensitised solar cells," *Progress in Photovoltaics*, vol. 15, no. 7, pp. 603–612, 2007.

[6] A. Islam, S. Prakash Singh, and L. Han, "Synthesis and application of new ruthenium complexes containing β-diketonato ligands as sensitizers for nanocrystalline TiO_2 solar cells," *International Journal of Photoenergy*, vol. 2011, Article ID 204639, 8 pages, 2011.

[7] J. Yu, Q. Li, J. Fan, and B. Cheng, "Fabrication and photovoltaic performance of hierarchically titanate tubular structures self-assembled by nanotubes and nanosheets," *Chemical Communications*, vol. 47, no. 32, pp. 9161–9163, 2011.

[8] M. K. Nazeeruddin, P. Péchy, T. Renouard et al., "Engineering of efficient panchromatic sensitizers for nanocrystalline TiO_2-based solar cells," *Journal of the American Chemical Society*, vol. 123, no. 8, pp. 1613–1624, 2001.

[9] S. Ito, H. Matsui, K. I. Okada et al., "Calibration of solar simulator for evaluation of dye-sensitized solar cells," *Solar Energy Materials and Solar Cells*, vol. 82, no. 3, pp. 421–429, 2004.

[10] J. Yu, J. Fan, and K. Lv, "Anatase TiO_2 nanosheets with exposed (001) facets: improved photoelectric conversion efficiency in dye-sensitized solar cells," *Nanoscale*, vol. 2, no. 10, pp. 2144–2149, 2010.

[11] J. Yu, J. Fan, and L. Zhao, "Dye-sensitized solar cells based on hollow anatase TiO_2 spheres prepared by self-transformation method," *Electrochimica Acta*, vol. 55, no. 3, pp. 597–602, 2010.
[12] L. Han, N. Koide, Y. Chiba, and T. Mitate, "Modeling of an equivalent circuit for dye-sensitized solar cells," *Applied Physics Letters*, vol. 84, no. 13, pp. 2433–2435, 2004.